

Effects of Sample Preparation Method and Thermal History on Phase Transition in Highly Asymmetric Block Copolymer: Comparison with Symmetric Block Copolymers

Soobum Choi, Nitin Y. Vaidya, and Chang Dae Han*

Department of Polymer Engineering, The University of Akron, Akron, Ohio 44325

Norihiro Sota and Takeji Hashimoto*

Department of Polymer Chemistry, Graduate School of Engineering, Kyoto University, Kyoto 606-8501, Japan

Received February 18, 2003

ABSTRACT: Symmetric and highly asymmetric polystyrene-*block*-polyisoprene-*block*-polystyrene (SIS triblock) copolymers were synthesized via sequential anionic polymerization using difunctional initiator, and symmetric and highly asymmetric polystyrene-*block*-polyisoprene (SI diblock) copolymers were also synthesized using monofunctional initiator. The molecular weight of the triblock copolymer was approximately twice that of the diblock copolymer. The phase transition temperatures of the SIS triblock and SI diblock copolymers were determined using oscillatory shear rheometry and small-angle X-ray scattering (SAXS), respectively. It has been found that the sample preparation methods (solvent casting vs compression molding) and annealing conditions employed have a profound influence on the “apparent” phase transition temperatures of the highly asymmetric block copolymers that undergo order–disorder transition (ODT) involving lattice disordering/ordering transition (LDOT) followed by the demicellization/micellization transformation (DMT) process, but little effect on the ODT temperature (T_{ODT}), where transition occurs between the ordered lamellae or cylinders and micelle-free disordered state with only thermal composition fluctuations, for the symmetric or nearly symmetric block copolymers. It has been observed, via transmission electron microscopy and SAXS, that highly asymmetric SIS triblock and SI diblock copolymers form thermodynamically stable disordered micelles between T_{ODT} and DMT temperature (T_{DMT}), and the disordered micelles transform into the micelle-free homogeneous state only with thermally induced composition fluctuations at temperatures above T_{DMT} . It has been found that T_{DMT} is much higher than T_{ODT} , that the T_{ODT} of symmetric SIS triblock copolymer is 24 ± 2 °C higher than that of the corresponding SI diblock copolymer, and that the T_{DMT} of highly asymmetric SIS triblock copolymer is 23 ± 2 °C higher than that of the corresponding SI diblock copolymer.

1. Background

During the past 2 decades a number of research groups have reported on phase transitions in block copolymers. Block copolymers may have different architectures (e.g., linear, tapered, or star-shaped). Theory predicting phase transition temperatures of linear AB-type diblock and ABA-type triblock copolymers is well documented.^{1–6} There have been numerous experimental studies reported on order–disorder transition (ODT) in linear AB-type diblock or ABA-type triblock copolymers. There are too many papers to cite them all here and the interested readers are referred to a review article.⁷ It should be mentioned that ODT is thermally reversible, and a block copolymer is in the homogeneous state with only thermally induced composition fluctuations at temperatures above ODT temperature (T_{ODT}).

Of particular interest is a comparison of T_{ODT} between ABA-type triblock and AB-type diblock copolymers. To facilitate our discussion later in this paper, in Figure 1a we present a comparison of theoretical phase diagrams,³ plots of χN vs f , for AB-type diblock copolymer¹ and for ABA-type triblock copolymer.^{3,4} In Figure 1, χ denotes the Flory–Huggins interaction parameter, N denotes the degree of polymerization, and f denotes the volume fraction of block A. Referring to Figure 1a, half of the N values for the triblock copolymer are used to prepare curve 1. It is seen in Figure 1a that the

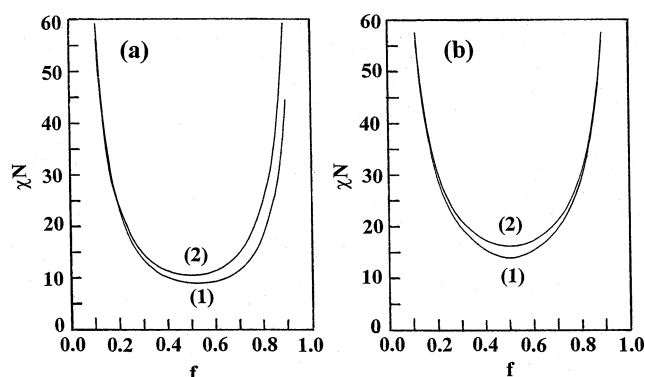


Figure 1. (a) Phase diagrams in terms of χN vs f from random phase approximation theory: curve 1 for ABA-type triblock copolymers and curve 2 for AB-type diblock copolymers. (b) Phase diagrams in terms of χN vs f from self-consistent mean field theory of Helfand and Wasserman: curve 1 for ABA-type triblock copolymers and curve 2 for AB-type diblock copolymers.

difference in χN (thus the difference in T_{ODT} , ΔT_{ODT}) between triblock copolymer and diblock copolymer depends on f ; namely, ΔT_{ODT} monotonically increases as the value of f increases. That is, according to Figure 1a, the phase diagram for ABA-type triblock copolymer is asymmetric, while the phase diagram for AB-type diblock copolymer is symmetric with respect to $f = 0.5$. Figure 1b shows theoretical phase diagrams from the

* Corresponding author.

Helfand–Wasserman theory² for both the AB-type diblock copolymer and the ABA-type triblock copolymer. It is seen in Figure 1b that ΔT_{ODT} is the largest at $f = 0.5$ and decreases as the value of f decreases or increases from 0.5, showing symmetry with respect to $f = 0.5$. What is common in parts a and b of Figure 1 is that the T_{ODT} of symmetric ($f = 0.5$) triblock copolymers is higher than that of the corresponding diblock copolymers, and highly asymmetric ($f < 0.2$) triblock and diblock copolymers have virtually an identical T_{ODT} , i.e., $\Delta T_{\text{ODT}} \approx 0$. To date, very few experimental studies have been reported, verifying the theoretical predictions for the highly asymmetric triblock and diblock copolymers. This is attributable to the practical difficulty with synthesizing an ABA-type triblock copolymer whose molecular weight is exactly twice that of an AB-type diblock copolymer.

It should be pointed out that the ODT described in theoretical studies^{1–6} involves the phase transition in AB-type diblock or ABA-type triblock copolymers from an ordered phase (alternating layers of lamellae, hexagonally packed cylinders, or spheres in a body-centered lattice) to the disordered (homogeneous) phase with thermally induced composition fluctuations. However, it will be clarified later in this paper that highly asymmetric block copolymers actually undergo ODT involving lattice disordering/ordering transition (LDOT), so that disordered spherical microdomains (or disordered micelles) with short-range order, instead of the disordered homogeneous phase, exist at temperatures above T_{ODT} as defined in theoretical studies.^{1–6} Thus we are of the opinion that for highly asymmetric block copolymers, the nature of the disordered phase in theoretically treated systems is different from that in the real systems. Nevertheless, in this paper we shall compare the ΔT_{ODT} s between triblock copolymer and diblock copolymer predicted in theoretical studies with those determined experimentally in this study and also in the literature.^{8–11}

Gehlsen et al.⁸ prepared nearly symmetric ($f = 0.55$) poly(ethylene-*alt*-propylene)-*block*-poly(ethylene)-*block*-poly(ethylene-*alt*-propylene) (PEP-*block*-PEE-*block*-PEP) and PEP-*block*-PEE copolymers, where f denotes the volume fraction of PEP block. They first synthesized, via anionic polymerization, *cis*-1,4-polyisoprene-*block*-1,2-polybutadiene, (1,4-PI)-*block*-(1,2-PB), copolymer and then coupled the diblock copolymer to obtain a triblock copolymer, (1,4-PI)-*block*-(1,2-PB)-*block*-(1,4-PI) copolymer, followed by hydrogenation. It is virtually impossible, via coupling reactions, to obtain 100% triblock copolymer. Thus, Gehlsen et al. applied fractionation to a mixture consisting of PEP-*block*-PEE and PEP-*block*-PEE-*block*-PEP copolymers. The fractionated PEP-*block*-PEE copolymer contained about 4 wt % PEP-*block*-PEE-*block*-PEP copolymer. They determined the T_{ODT} s of the fractionated, nearly symmetric PEP-*block*-PEE and PEP-*block*-PEE-*block*-PEP copolymers using isochronal dynamic temperature sweep experiments. They reported that the PEP-*block*-PEE-*block*-PEP copolymer had $T_{\text{ODT}} \approx 144$ °C and the PEP-*block*-PEE copolymer containing 4 wt % PEP-*block*-PEE-*block*-PEP copolymer had $T_{\text{ODT}} \approx 78$ °C, giving rise to $\Delta T_{\text{ODT}} = 66$ °C.

Riise et al.⁹ investigated ODT in symmetric polystyrene-*block*-polyisoprene-*block*-polystyrene (SIS triblock) and polystyrene-*block*-polyisoprene (SI diblock) copolymers. The molecular weight of the SIS triblock copoly-

mer was approximately twice that of the SI diblock copolymer. They reported that the SI diblock copolymer had $T_{\text{ODT}} = 130 \pm 1$ °C and the SIS triblock copolymer had $T_{\text{ODT}} = 152 \pm 2$ °C, giving rise to $\Delta T_{\text{ODT}} = 25$ °C. Notice that ΔT_{ODT} between the SIS triblock and SI diblock copolymers observed by Riise et al.⁹ is *not* as large as that between the PEP-*block*-PEE-*block*-PEP and PEP-*block*-PEE copolymers observed by Gehlsen et al.,⁸ but the trend that the T_{ODT} of symmetric triblock copolymer is higher than that of the corresponding diblock copolymer is consistent with the prediction of mean-field theory (see Figure 1). The measurements of T_{ODT} reported in the two studies referred to above were based on symmetric or nearly symmetric diblock and triblock copolymers. Therefore a comparison of ΔT_{ODT} between their experimental results with theoretical studies is reasonable, because ODT in those systems occur from lamellar microdomains directly into the homogeneous phase only with thermally induced composition fluctuations.

Adams et al.¹⁰ investigated ODT in highly asymmetric SIS triblock and SI diblock copolymers having a 0.13 weight fraction of polystyrene (PS) block using isochronal dynamic temperature sweep experiments at angular frequencies ranging from 0.015 to 3.9 rad/s. They prepared specimens for the rheological measurements by *compression molding*. They reported that the SI diblock copolymer (D78) had $T_{\text{ODT}} = 152 \pm 3$ °C and the SIS triblock copolymer (T149) had $T_{\text{ODT}} = 155 \pm 2$ °C, giving rise to $\Delta T_{\text{ODT}} = 3$ °C. According to Adams et al.,¹⁰ the molecular weight of T149 was approximately twice that of D78. The smaller value of $\Delta T_{\text{ODT}} = 3$ °C between the highly asymmetric triblock copolymer T149 and the highly asymmetric diblock copolymer D78 reported by Adams et al.,¹⁰ as compared to the larger value of $\Delta T_{\text{ODT}} = 22$ °C between the nearly symmetric SIS triblock and the nearly symmetric SI diblock copolymer reported by Riise et al.,⁹ appears to be consistent with the prediction of mean field theory (see Figure 1). However, as will be presented later in this paper, the sample preparation methods employed, *compression molding* vs *solvent casting*, have a profound influence on the observed “apparent” T_{ODT} of highly asymmetric block copolymers, while little influence on the T_{ODT} of symmetric or nearly symmetric block copolymers.

Ryu et al.¹¹ compared the T_{ODT} , which was determined from isochronal dynamic temperature sweep experiments at an angular frequency of 1.0 rad/s, of highly asymmetric SI diblock and SIS triblock copolymers, each having a 0.167 weight fraction of PS block. Like Adams et al.,¹⁰ Ryu et al.¹¹ also prepared specimens for the rheological measurements by *compression molding*. They reported that the SI diblock copolymer had $T_{\text{ODT}} = 200 \pm 2$ °C and the SIS triblock copolymer had $T_{\text{ODT}} = 225 \pm 2$ °C, giving rise to $\Delta T_{\text{ODT}} = 25$ °C, which is much larger than $\Delta T_{\text{ODT}} = 3$ °C reported by Adams et al.¹⁰ who also employed highly asymmetric SI diblock and SIS triblock copolymers, but it is virtually the same as that reported by Riise et al.⁹ who employed symmetric SIS and SI diblock copolymers. It is then fair to state that the existing experimental results are confusing.

It should be pointed out that the T_{ODT} or ΔT_{ODT} reported by Adams et al.¹⁰ and Ryu et al.¹¹ for highly asymmetric block copolymers correspond to LDOT temperature (T_{LDOT}) or ΔT_{LDOT} (the difference in T_{LDOT}

Table 1. Molecular Characteristics of the SIS Triblock and SI Diblock Copolymers Synthesized in This Study

sample code	M_n (g/mol) ^a	M_w/M_n ^b	w_{PS} ^c	f ^d	$T_{g,PS}$ (°C) ^e	$T_{g,PI}$ (°C) ^e
(a) Symmetric Block Copolymers						
SI-16	1.55×10^4	1.04	0.51	0.47	64	-61
SI-13	1.25×10^4	1.08	0.53	0.49	55	-62
SIS-26 ^f	2.58×10^4	1.11	0.53	0.49	56	-53
(b) Highly Asymmetric Block Copolymers						
SI-57	5.70×10^4	1.07	0.16	0.14	68	-56
SIS-110 ^f	1.06×10^5	1.04	0.16	0.14	69	-48

^a Number-average molecular weight (M_n) determined by membrane osmometry. ^b Polydispersity index determined by gel permeation chromatography. ^c Weight fraction of PS block (w_{PS}) determined by nuclear magnetic resonance spectroscopy. ^d Volume fraction of PS block (f) calculated at room temperature. Note that the value of f varies with temperature, because the temperature dependence of specific volumes of PS and PI are different. ^e Measured by DSC at a heating rate of 20 °C/min. ^f Synthesized using difunctional initiator.

between triblock copolymer and diblock copolymer).

Although phase transition in block copolymers has been reported by numerous research groups during the last two decades, little systematic study has been reported on the effects of sample preparation methods (compression molding vs solvent casting) and thermal history of highly asymmetric and/or symmetric block copolymers on phase transition temperature. This subject is very important when one wishes to compare ΔT_{ODT} between highly asymmetric triblock and diblock copolymers with that between symmetric or nearly symmetric triblock and diblock copolymers.

In this paper, we report on the effects of sample preparation methods (solvent casting vs compression molding) and thermal history on phase transition in highly asymmetric SIS triblock and SI diblock copolymers and then compare the results with those for nearly symmetric SIS triblock and SI diblock copolymers. For the study, we employed oscillatory shear rheometry, small-angle X-ray scattering (SAXS), and transmission electron microscopy (TEM).

2. Experimental Section

Synthesis of Polymers and Characterization. We synthesized, via sequential living anionic polymerization, SIS triblock copolymers (listed in Table 1) using difunctional initiator. For this, we first prepared difunctional initiator by purifying a precursor, 1,3-bis(phenylethenyl) benzene (PEB) (yellowish liquid), which was received from Dow Chemical Co. Specifically, PEB was purified by first dissolving the crude, viscous PEB in *n*-hexane as solvent and then by passing repeatedly the PEB/*n*-hexane solution through a thin layer chromatographic (TLC) column packed with activated silica gel with sizes between 230 and 400 mesh (Selecto Scientific) until only one spot in the TLC column was detected. The purified PEB/*n*-hexane solution was distilled under a high vacuum. Dilithium initiator (DLI) was prepared by reacting 2 mol of *sec*-butyllithium (*sec*-BuLi) with 1 mol of PEB in cyclohexane as solvent. The DLI thus obtained was analyzed, via proton nuclear magnetic resonance (¹H NMR) spectroscopy, to confirm the molecular structure and completeness of the addition reaction. Pentamethyldiethylenetriamine (PMDETA) (Aldrich) needed to obtain narrow molecular weight polyisoprene (PI) was purified by vacuum distillation in the presence of calcium hydride. PMDETA with a mole ratio of 0.18/1 for *sec*-BuLi was added to the reactor using a syringe. The reactor was then purged with argon gas and heated, while stirring, to 55 °C using a water bath. When the temperature of the water bath reached about 55 °C, DLI and PMDETA were added to first polymerize the isoprene monomer. About 2 h

after the addition of DLI, styrene monomer was added to the reactor. After the copolymerization of isoprene and styrene monomers for 1.5 h, a small amount of degassed methanol was added to terminate the living polymerization, at which point the color of the solution changed from yellowish red to colorless. Then the reactor temperature was lowered to room temperature, and the solution was precipitated by addition of an excess amount of methanol. The precipitated polymer was filtered and dried at room temperature for 3 days in a fume hood and then at 60 °C for 12 h in a vacuum oven.

Also, we synthesized, via sequential living anionic polymerization, nearly symmetric SI diblock copolymers (listed in Table 1) using monofunctional initiator. For the polymerization, cyclohexane was used as the solvent, and *sec*-BuLi was used as initiator to first polymerize the isoprene monomer at room temperature for 10 h and then to copolymerize styrene monomer with this living poly(isoprenyl) lithium at room temperature for 12 h. For this, styrene was first stirred over freshly crushed calcium hydride (Aldrich) for 3 days and then vacuum distilled in the presence of dibutylmagnesium prior to use. Cyclohexane was stirred over calcium hydride for 1 week and then vacuum distilled into a flask containing sodium. Injecting a small amount of degassed methanol using a syringe terminated the living polymerization, at which point the color of the solution in the flask changed from yellowish red to colorless. The solution was precipitated by addition of an excess amount of methanol. The precipitated polymer was filtered and dried for 3 days at room temperature in a hood and finally dried at 60 °C for 12 h under vacuum.

Membrane osmometry (Jupiter Instrument) was used to determine the number-average molecular weight (M_n) and gel permeation chromatography (GPC) (Waters) to determine the polydispersity index (M_w/M_n) of each block polymer synthesized. Block copolymer composition was determined using ¹H NMR spectroscopy. Table 1 gives a summary of sample codes and the molecular characteristics of the block copolymers.

Sample Preparation. Samples for oscillatory shear rheometry, SAXS, and TEM were prepared by first dissolving a predetermined amount of block copolymer in toluene (10 wt % in solution) in the presence of 0.1 wt % antioxidant (Irganox 1010, Ciba-Geigy Group) and then slowly evaporating the solvent. The evaporation of solvent was carried out initially in a fume hood slowly at room temperature for 1 week and then in a vacuum oven at 40 °C for 3 days. The last trace of solvent was removed by drying the samples in a vacuum oven at an elevated temperature by gradually raising the temperature about 20 °C above the glass transition temperature of each block copolymer. The drying of the samples was continued until there was no further change in weight and then the specimens were stored in a refrigerator. Prior to oscillatory shear rheometry, SAXS, or TEM, the solvent cast samples were thermally treated under predetermined conditions, which were specific to each block copolymer. The details of the thermal treatment for each sample will be described below when the experimental results are presented. To investigate the effect of sample preparation methods on phase transition temperature of the block copolymers synthesized in this study, we employed, as well, compression molding to prepare samples. In preparing a compression-molded specimen, about 1.5 g of a dried block copolymer sample in the form of powder was placed into a round cavity having the diameter of 25 mm and the depth of 2 mm. The sample was then pressed by placing a round object having a weight of 2.66 kg on top of the specimen. Specifically, SI-16 specimens were compression molded at 120 °C for 20 min, and SIS-110 specimens were compression molded at 150 °C for 20 min. It should be mentioned that the temperature employed for compression molding SI-16 specimens was above its T_{ODT} and the temperature employed for compression molding SIS-110 specimens was below its T_{LDOT} , as will be clarified later in this paper. The compression-molded specimen was quenched rapidly from the respective temperatures in ice–water. The applied pressure is estimated to have been 9.99 kPa (1.45 psi). Such a low pressure applied to the specimen would have affected little the phase behavior of the block copolymer specimen had it been annealed for a suf-

ficiently long period to relieve the stresses accumulated during compression molding followed by a rapid quenching. This will be elaborated on later in this paper. The phase behavior of a compression-molded block copolymer would have been much more affected had a very high-pressure been applied during specimen preparation. We compared the phase transition temperature of the samples prepared by compression molding with that prepared by solvent casting.

Oscillatory Shear Rheometry. An Advanced Rheometric Expansion System (ARES, Rheometric Scientific) was used in the oscillatory mode with parallel plate fixtures (25 mm diameter). Dynamic frequency sweep experiments were conducted, i.e., the dynamic storage modulus (G') and dynamic loss modulus (G'') were measured as functions of angular frequency (ω) ranging from 0.01 to 100 rad/s at various temperatures during heating. The temperature increment in the frequency sweep experiment varied from 3 to 10 °C and the specimen was kept at a constant temperature for 30–40 min before rheological measurements actually began. Data acquisition was accomplished with the aid of a microcomputer interfaced with the rheometer. The temperature control was satisfactory to within ± 1 °C. For the rheological measurements, the strain was varied from 0.03 to 0.3 depending upon the measurement temperature, which was well within the linear viscoelastic range for the materials investigated. Dynamic temperature sweep experiments under isochronal conditions were also conducted, i.e., G' was measured at $\omega = 0.01$, 0.1, 1.0, or 2.0 rad/s during heating. All experiments were conducted under a nitrogen atmosphere to preclude oxidative degradation of the samples.

Small-Angle X-ray Scattering (SAXS) Experiment. SAXS experiments were conducted under a nitrogen atmosphere in the heating and cooling processes, using an apparatus described in detail elsewhere,^{12,13} which consists of an 18 kW rotating-anode X-ray generator operated at 40 kV \times 300 mA (MAC Science Co. Ltd., Yokohama, Japan), a graphite crystal for incident-beam monochromatization, a 1.5-m camera, and a one-dimensional position-sensitive proportional counter. The Cu K α line ($\lambda = 0.154$ nm) was used. The SAXS profiles were measured as a function of temperature and were corrected for absorption, air scattering, slit-height, and slit-width smearing.¹⁴ The absolute SAXS intensity was obtained using the nickel-foil method.¹⁵ The temperature of the SAXS experiment was controlled using a specially constructed enclosure that was sealed by nitrogen gas. This temperature enclosure and controller enabled us to maintain variations in sample temperature to within ± 0.002 °C. A specimen was exposed to the X-ray beam to measure SAXS profiles for the period (typically for 30 min) after holding for 30 min at each temperature increment during the heating process or at each temperature decrement during the cooling process.

Transmission Electron Microscopy (TEM). The morphology of a highly asymmetric diblock copolymer (SI-57) and a highly asymmetric SIS triblock copolymer (SIS-110) was investigated via TEM. The ultrathin sectioning was performed by cryoultramicrotomy at -100 °C using a diamond knife, which was below the glass transition temperature ($T_g = -68$ °C) of PI to attain specimen rigidity, using a Reichert Ultracut S low-temperature sectioning system. A transmission electron microscope (JEM1200EX II, JEOL) operated at 120 kV was used to record the morphology of the specimens stained with osmium tetroxide vapor. The thermal histories of the specimens used for TEM experiments will be described below when TEM images are presented.

3. Results and Discussion

Effect of Sample Preparation Method on Phase Transitions in Symmetric and Highly Asymmetric Block Copolymers. Figure 2 describes the effect of the sample preparation methods employed, compression molding and solvent casting, on the temperature dependence of dynamic storage modulus (G'), during heating, in the isochronal temperature sweep experi-

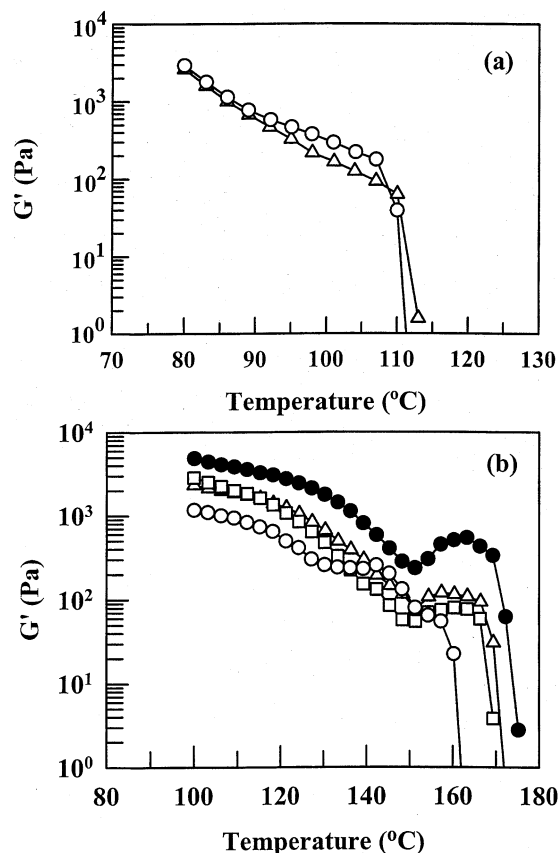


Figure 2. Temperature dependence of dynamic storage modulus G' during heating in the isochronal temperature sweep experiment at $\omega = 0.01$ rad/s: (a) symmetric SI-16 specimens prepared by compression molding at 120 °C for 20 min (Δ) and by solvent casting followed by an isothermal annealing at 92 °C for 3 days with rapid quenching in ice water (\circ); (b) highly asymmetric SIS-110 specimens prepared by solvent casting followed by isothermal annealing at 85 °C for 5 days (\circ), by compression molding at 150 °C for 20 min (\bullet), by compression molding at 150 °C for 20 min, followed by isothermal annealing at 85 °C for 2 days (Δ), and by compression molding at 150 °C for 20 min, followed by isothermal annealing at 85 °C for 3 days (\square).

ments at an angular frequency (ω) of 0.01 rad/s for (a) a symmetric diblock copolymer SI-16 and (b) a highly asymmetric triblock copolymer SIS-110. Referring to Figure 2a, one specimen of SI-16 was prepared by compression molding at 120 °C for 20 min under vacuum (Δ) and another specimen of SI-16 was prepared by solvent casting followed by isothermal annealing at 92 °C for 3 days (\circ). Following the rheological criterion that the temperature at which values of G' begin to drop precipitously during the isochronal dynamic temperature sweep experiment may signify the onset of ODT in symmetric or nearly symmetric block copolymers,¹⁶ from Figure 2a we determine the T_{ODT} of SI-16 to be ca. 110 °C, regardless of whether the specimen was prepared by compression molding or solvent casting. Referring to Figure 2b, one specimen of SIS-110 was prepared by solvent casting followed by an isothermal annealing at 85 °C for 5 days, and another specimen of SIS-110 was prepared by compression molding at 150 °C for 20 min. Subsequently, the compression-molded specimens were annealed in a vacuum oven at 85 °C for 2 or 3 days and then each of the annealed specimens was subjected to isochronal dynamic temperature sweep experiment. The following observations are worth noting in Figure 2b. Over the entire range of temperatures

tested, (i) the compression molded specimen *without* an isothermal annealing (●) has larger values of G' compared to other specimens, and the G' goes through a large minimum at ca. 150 °C followed by a rapid increase and then begins to drop precipitously at ca. 170 °C and has very small values at ca. 175 °C, (ii) the G' of the compression-molded specimen after an isothermal annealing at 85 °C for 2 days (△) goes through a mild minimum at ca. 150 °C followed by a rapid increase and then begins to drop precipitously at ca. 168 °C and has very small values at ca. 172 °C, (iii) the G' of the compression molded specimen after an isothermal annealing at 85 °C for 3 days (□) also goes through a mild minimum at ca. 150 °C followed by a rapid increase and then begins to drop precipitously at ca. 168 °C and has very small values at ca. 170 °C, and (iv) the G' of the solvent-cast specimen after an isothermal annealing at 85 °C for 5 days (○) goes through a mild minimum at ca. 135 °C and then begins to drop precipitously at ca. 161 °C and has very small values at ca. 162 °C. Interpretation of the temperature at which values of G' begin to drop precipitously for the highly asymmetric SIS-110 shown in Figure 2b, will follow presentation of the SAXS and dynamic frequency sweep experiments at various temperatures, below.

It is very clear from Figure 2b that the sample preparation methods employed, compression molding or solvent casting, have a profound influence on the temperature at which values of G' begin to drop precipitously for the highly asymmetric triblock copolymer SIS-110. It is particularly noteworthy that isothermal annealing of compression-molded SIS-110 specimens brought the temperature at which values of G' begin to be negligibly small, to lower values toward the temperature determined from a solvent-cast specimen which had been isothermally annealed.

It should be mentioned that we did not add an antioxidant to compression-molded specimens, whereas an antioxidant was added to all solvent-cast specimens employed in this study. We found that in the *absence* of an antioxidant, a compression-molded SIS-110 specimen underwent thermal degradation after annealing at 85 °C for a period longer than 3 days, which then resulted in, during the isochronal dynamic temperature sweep experiment, values of G' lower than those of the solvent-cast specimen. Thus, we concluded that it was not possible to attain equilibrium morphology for compression-molded SIS-110 specimens by annealing at 85 °C for a sufficiently long period (longer than 3 days) without encountering thermal degradation. What is clear in Figure 2b, however, is that the temperature at which values of G' begin to be negligibly small during the isochronal dynamic temperature sweep experiments of compression-molded SIS-110 specimens, decreases from 175 to 172 °C after annealing for 2 days (△ in Figure 2b), and then to 170 °C after annealing for 3 days (□ in Figure 2b). These temperatures are still higher than the corresponding temperature (162 °C) obtained from a solvent-cast specimen which was annealed for 5 days (○ in Figure 2b). The above experimental results seem reasonable, because a compression-molded specimen must have had some accumulated stresses and the alignment imposed by the flow during compression molding would have apparently affected the dynamic mechanical behavior of highly asymmetric block copolymers, i.e., the compression-molded specimen was in a nonequilibrium state. During isothermal

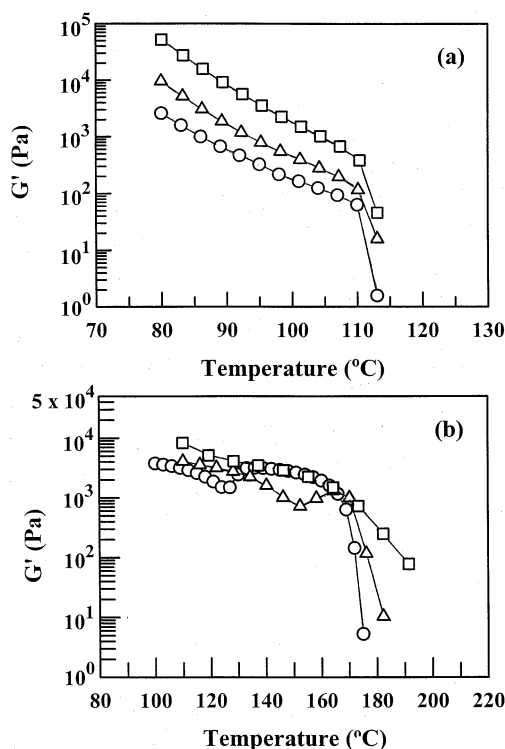


Figure 3. Temperature dependence of dynamic storage modulus G' during heating in the isochronal temperature sweep experiment at three different angular frequencies: (○) $\omega = 0.01$ rad/s; (△) $\omega = 0.1$ rad/s; (□) $\omega = 1$ rad/s for (a) symmetric SI-16 specimens that were compression molded at 120 °C for 20 min and (b) highly asymmetric SIS-110 specimens that were compression molded at 150 °C for 20 min,

annealing for 2 or 3 days, the stresses built in the compression-molded specimen would have been relaxed somewhat and the microdomain structure, especially grain boundary structure, would have been accordingly rearranged. Earlier, Adams et al.¹⁰ and Ryu et al.¹¹ prepared specimens of highly asymmetric SI diblock and SIS triblock copolymers by compression molding and conducted isochronal dynamic temperature sweep experiments of the specimens *without* isothermal annealing to determine a phase transition temperature.

The effect of applied angular frequency on the temperature dependence of G' , during heating, in the isochronal temperature sweep experiments for compression-molded specimens are presented in Figure 3a for a nearly symmetric diblock copolymer SI-16 and in Figure 3b for a highly asymmetric triblock copolymer SIS-110. Referring to Figure 3, the specimens of SI-16 were prepared by compression molding at 120 °C for 20 min under vacuum and the specimens of SIS-110 were prepared by compression molding at 150 °C for 20 min under vacuum. From Figure 3a we determine the T_{ODT} of SI-16 to be ca. 110 °C, regardless of the values of the applied ω (0.01, 0.1, or 1.0 rad/s). On the other hand, in Figure 3b we observe that the applied values of ω have a profound influence on the temperature dependence of G' for SIS-110: namely, (i) at $\omega = 0.01$ rad/s, values of G' (○) go through a large minimum at ca. 125 °C, increase rapidly followed by a broad maximum, and finally decrease very rapidly at ca. 170 °C; (ii) at $\omega = 0.1$ rad/s, values of G' (△) go through a large minimum at ca. 153 °C, increase rapidly followed by a maximum, and finally decrease very rapidly at ca. 175 °C; (iii) at $\omega = 1$ rad/s, values of G' (□) decrease gradually without showing any particular temperature at which G' drops

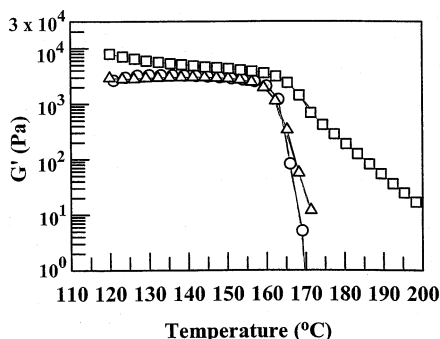


Figure 4. Temperature dependence of dynamic storage modulus G' during heating in the isochronal temperature sweep experiment for highly asymmetric solvent-cast SIS-110 specimens, which were annealed at 110 °C for 3 days, at three different angular frequencies: (○) $\omega = 0.01$ rad/s; (△) $\omega = 0.1$ rad/s; (□) $\omega = 1$ rad/s.

precipitously. The above observations suggest that the compression-molded highly asymmetric SIS-110 specimens underwent further annealing during the isochronal dynamic temperature sweep experiment. Below we will explain the origin of a minimum in G' observed in Figure 3b.

Figure 4 describes the effect of applied angular frequency on the temperature dependence of G' , during heating, in the isochronal temperature sweep experiment for highly asymmetric SIS-110 specimens that were prepared by solvent casting followed by isothermal annealing at 110 °C for 3 days. In contrast to the results of compression-molded specimens presented in Figure 3b, in Figure 4 we observe that values of G' do *not* go through a minimum during the isochronal dynamic temperature sweep experiments at all three values of applied ω (0.01, 0.01, and 1.0 rad/s) and that values of G' begin to drop precipitously at ca. 160 °C for $\omega = 0.01$ and 0.1 rad/s, but decrease gradually with increasing temperature for $\omega = 1$ rad/s. From Figures 3b and 4, we conclude that the sample preparation methods employed have a profound influence on the temperature dependence of G' in the isochronal dynamic temperature sweep experiments for the highly asymmetric triblock copolymer SIS-110.

Earlier, Sakamoto et al.¹⁷ made similar experimental observations, who employed a cylinder-forming SIS triblock copolymer (with a 0.183 weight fraction of PS and a molecular weight of 1.4×10^5) (Vector 4111, Dexco Polymer Company). Specifically, their SAXS experiments revealed that Vector 4111 underwent order-order transition (OOT) at 179–185 °C with (i) hexagonally packed cylindrical microdomains of PS at $T \leq 179$ °C, (ii) the coexistence of cylindrical and spherical microdomains of PS at 180 °C $\leq T \leq 185$ °C, (iii) spherical microdomains in body centered cubic (bcc) lattice of PS at 185 °C $< T \leq 210$ °C and (iv) the cubic lattice of the spheres was distorted with a further increase in temperature so that ODT involving the lattice disordering transition occurred at temperatures between 210 (onset) and 214 °C (completion) and the spherical microdomain structure of PS with a liquidlike short-range order persisted even up to 220 °C, the highest experimental temperature employed. TEM revealed that (i) at 170 °C, Vector 4111 had hexagonally packed cylindrical microdomains of PS, (ii) at 185 °C, cylindrical and spherical microdomains of PS coexisted, and (iii) as the temperature was increased further to 220 °C, only spherical microdomains of PS persisted;

i.e., the T_{DMT} of Vector 4111 was higher than 220 °C. The specimens in their study were prepared by solvent casting followed by an isothermal annealing at 140 °C for 2 days. Sakamoto et al.¹⁷ noted that the depth of G' minimum observed, during heating, in the isochronal dynamic temperature sweep experiment was very large at $\omega = 0.01$ rad/s, but it decreased considerably at $\omega = 0.1$ rad/s. Again, they found that the applied ω had a significant effect on the temperature dependence of G' for highly asymmetric triblock copolymer Vector 4111 during isochronal dynamic temperature sweep experiments. Independently, using a highly asymmetric SI diblock copolymer (SI-60) (with a 0.17 weight fraction of PS and a molecular weight of 6.0×10^4) and also a highly asymmetric SIS triblock copolymer (SIS-120) (with a 0.17 weight fraction of PS and a molecular weight of 1.2×10^5), Ryu et al.¹¹ conducted isochronal dynamic temperature sweep experiments at $\omega = 1$ rad/s. The specimens in their study were prepared by compression molding. According to Ryu et al.,¹¹ both block copolymers had hexagonally packed cylindrical microdomains of PS at room temperature and they underwent, during heating, OOT into spherical microdomains in bcc lattice of PS before undergoing ODT. The isochronal dynamic temperature sweep experiments of Ryu et al.¹¹ showed that values of G' first decreased, went through a minimum, followed by a rapid increase, and then decreased rapidly. They attributed the existence of a minimum in G' to the onset of OOT.

We wish to point out the differences in the origin of a minimum of G' observed in the isochronal dynamic temperature sweep experiments between the present study (Figures 2b and 3b) and the previous studies of Sakamoto et al.¹⁷ and Ryu et al.¹¹ The minimum in G' appearing in both Figures 2a and 3b originated from the annealing effects involving softening and ordering (perfection) of bcc-spheres, which strongly depends on the specimen preparation methods employed (compare Figure 3b with Figure 4) and the applied angular frequency. On the other hand, a minimum in G' was observed, regardless of the sample preparation methods employed (compression molding vs solvent casting) and the applied angular frequency, in the isochronal dynamic temperature sweep experiments conducted by Sakamoto et al.¹⁷ and Ryu et al.¹¹ The observed minimum in G' in those studies occurred due to the phase transition OOT.

Effect of Thermal History on Phase Transition in Highly Asymmetric SIS Triblock Copolymer SIS-110. Figure 5 describes the effect of the thermal history of solvent-cast highly asymmetric SIS-110 specimens on the temperature dependence of G' , during heating, in the isochronal dynamic temperature sweep experiments at $\omega = 0.01$ rad/s. The experiments were conducted to determine optimum annealing conditions for the dynamic frequency sweep experiments and also for SAXS experiments for SIS-110. The following observations are worth noting in Figure 5. When the specimen was annealed at 85 °C for 10 days (○), during the isochronal dynamic temperature sweep experiment, values of G' go through a minimum at ca. 116 °C and then increase rapidly followed by a gradual decrease until reaching ca. 165 °C, at which values of G' begin to drop precipitously. However, when the specimen was annealed at 110 °C for 3 days (△), during the isochronal dynamic temperature sweep experiment, values of G' decrease initially very slowly until reaching ca. 116 °C

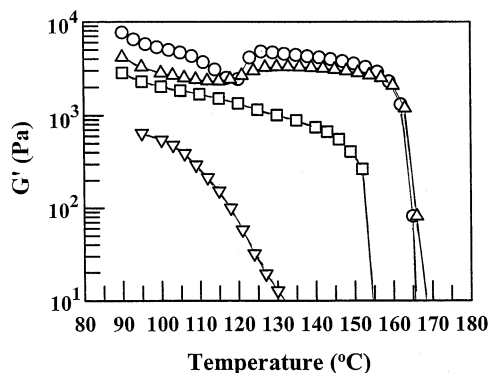


Figure 5. Temperature dependence of dynamic storage modulus G' during heating in the isochronal temperature sweep experiment at $\omega = 0.01$ rad/s for highly asymmetric solvent-cast SIS-110 specimens, which received different thermal treatments prior to experiment: (○) after annealing at 85 °C for 10 days; (Δ) after annealing at 110 °C for 3 days; (□) after annealing at 110 °C for 7 days; (▽) after annealing at 120 °C for 3 days.

at which values of G' begin to increase very slowly, and then stay more or less constant until reaching ca. 165 °C at which G' begins to drop precipitously. It is interesting to observe in Figure 5 that the temperature at which values of G' begin to drop precipitously is virtually identical whether a specimen was annealed at 85 °C for 10 days or at 110 °C for 3 days, but the minimum in G' virtually disappears when an SIS-110 specimen was annealed at 110 °C for 3 days. In a previous paper,¹⁸ Yamaguchi et al. reported that a minimum in G' observed for a highly asymmetric, sphere-forming SI diblock copolymer during isochronal dynamic temperature sweep experiments disappeared when the specimen was annealed for a sufficiently long time. They presented experimental results of SAXS and TEM, demonstrating that sufficiently long annealing perfected the ordered structure of the highly asymmetric SI diblock copolymer. However, we must await more information from SAXS and TEM before concluding whether the appearance of a minimum in G' in Figure 5 for SIS-110 is attributable to an annealing effect or OOT. As mentioned above, the appearance of a minimum in G' in the isochronal dynamic temperature sweep experiment for cylinder-forming block copolymers often signifies the onset of OOT.^{11,17,19,20}

Also shown in Figure 5 are the results of the isochronal dynamic temperature sweep experiments at $\omega = 0.01$ rad/s when an SIS-110 specimen was annealed at 110 °C for 7 days (□) or at 120 °C for 3 days (▽). In Figure 5, we observe that (i) when a specimen was annealed at 110 °C for 7 days, G' does not go through a minimum and begins to drop precipitously at ca. 154 °C, which is ca. 11 °C lower than the temperature at which G' begins to drop precipitously when a specimen was annealed at 110 °C for 3 days (Δ) and that (ii) when a specimen was annealed at 120 °C for 3 days, G' decreases steadily with increasing temperature without showing any particular temperature at which G' begins to drop precipitously.

To find the origin of the different temperature dependence of G' on the thermal history of SIS-110 specimens, we measured the molecular weight and polydispersity index, via GPC, of each specimen after the thermal treatment. We made the following observations: (i) the molecular weight ($M_w = 91\,700$) of the specimen annealed at 110 °C for 3 days decreased slightly (ca. 4%)

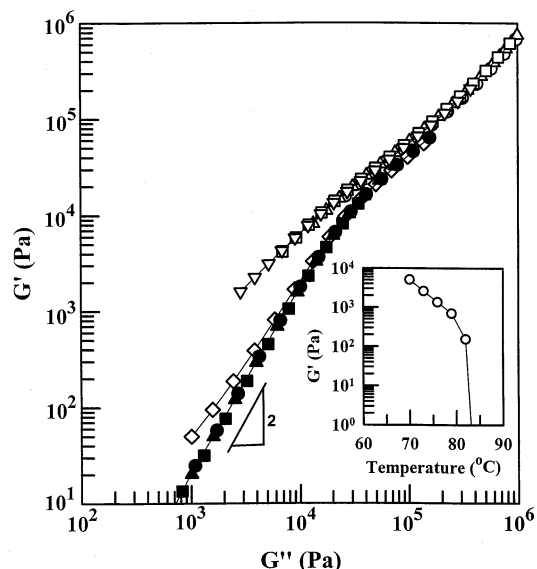


Figure 6. Log G' vs log G'' plots for a symmetric solvent-cast SI-13 specimen during heating at various temperatures: (○) 70 °C; (Δ) 73 °C; (□) 76 °C; (▽) 80 °C; (◇) 83 °C; (●) 86 °C; (▲) 90 °C; (■) 95 °C. The inset at the lower right-hand side describes variations of G' with temperature during isochronal dynamic temperature sweep experiments of a solvent-cast SI-13 specimen at $\omega = 0.01$ rad/s. Prior to the rheological measurements, the specimen was annealed at 80 °C for 2 days.

compared to that ($M_w = 94\,900$) annealed at 85 °C for 10 days with little change in polydispersity index (1.13 vs 1.12); (ii) the molecular weight ($M_w = 81\,000$) of the specimen annealed 110 °C for 7 days decreased considerably (ca. 15%) compared to that ($M_w = 94\,900$) annealed at 85 °C for 10 days and the polydispersity index increased from 1.12 to 1.27; (iii) the molecular weight ($M_w = 77\,000$) of the specimen annealed 120 °C for 3 days decreased further (ca. 19%) compared to that ($M_w = 94\,900$) annealed at 85 °C for 10 days and the polydispersity index increased from 1.12 to 1.31. Thus, we conclude that the different temperature dependence of G' observed in Figure 5 originated from changes in molecular weight and polydispersity index of the SIS-110 specimens. Therefore, in the subsequent dynamic frequency sweep experiments and SAXS study, SIS-110 specimens were annealed at 110 °C for 3 days.

Difference in T_{ODT} Between Symmetric SI Diblock and SIS Triblock Copolymers. For the reasons that will be clear below, we have decided to determine the T_{ODT} of the symmetric SI-13 and SIS-26 using log G' vs log G'' plots. As given in Table 1, the molecular weight of SI-13 is almost half the molecular weight of SIS-26. Figure 6 gives log G' vs log G'' plots at various temperatures, during heating, ranging from 70 to 95 °C for a solvent-cast SI-13 specimen, which was annealed at 80 °C for 2 days. The inset on the lower right side of Figure 6 describes the results of the isochronal dynamic temperature sweep experiment at $\omega = 0.01$ rad/s. It is seen in Figure 6 that the log G' vs log G'' plot makes a sudden shift downward at 83 °C (◇), another small shift downward at 86 °C (●) with a slope close to 2 in the terminal region, and the log G' vs log G'' plots at 90 and 95 °C overlap with that at 86 °C. Following the rheological criterion of Han et al.,²¹ from the log G' vs log G'' plots in Figure 6 we determine the T_{ODT} of SI-13 to be ca. 86 °C, which is very close to the temperature at which values of G' begin to drop precipitously in the

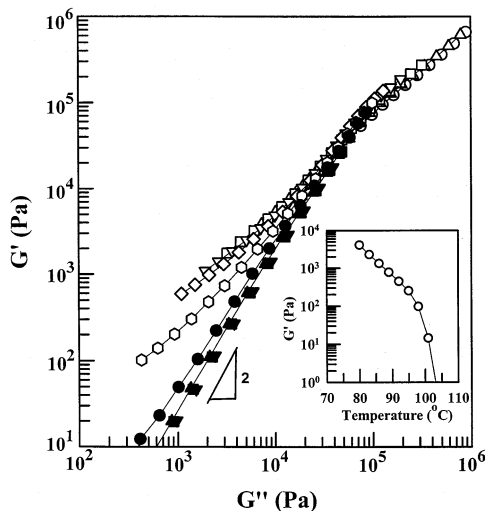


Figure 7. Log G' vs log G'' plots for a symmetric solvent-cast SIS-26 specimen during heating at various temperatures: (○) 80 °C; (△) 85 °C; (□) 90 °C; (▽) 93 °C; (◇) 96 °C; (○) 100 °C; (●) 103 °C; (▲) 106 °C; (■) 110 °C; (▼) 113 °C. The inset at the lower right-hand side describes variations of G' with temperature during isochronal dynamic temperature sweep experiments of a solvent-cast SIS-26 specimen at $\omega = 0.01$ rad/s. Prior to the rheological measurements, the specimen was annealed at 85 °C for 3 days.

isochronal dynamic temperature sweep experiment (see the inset).

Figure 7 gives log G' vs log G'' plots at various temperatures, during heating, ranging from 80 to 113 °C for a solvent-cast SIS-26 specimen, which was annealed at 85 °C for 3 days. The inset on the lower right side of Figure 7 describes the results of the isochronal dynamic temperature sweep experiment at $\omega = 0.01$ rad/s. From the log G' vs log G'' plots in Figure 7 we determine the T_{ODT} of SIS-26 to be ca. 106 °C, which is very close to the temperature at which values of G' begin to drop precipitously in the isochronal dynamic temperature sweep experiment (see the inset). From Figures 6 and 7 we conclude that the T_{ODT} of SIS-26 is about 20 °C higher than that of SI-13. This finding is very close to that ($\Delta T_{\text{ODT}} = 22$ °C) reported earlier by Riise et al.,⁹ who also employed symmetric SIS triblock and SI diblock copolymers.

Difference in Phase Transition Temperature Between Highly Asymmetric SI Diblock and SIS Triblock Copolymers. (a) Phase Transition in Highly Asymmetric SI Diblock Copolymer SI-57. Figure 8 describes the results of the isochronal dynamic temperature sweep experiment at $\omega = 0.01$ rad/s for highly asymmetric solvent-cast SI-57 specimens that received different thermal treatments. The following observations are worth noting in Figure 8. For the specimen annealed at 70 °C for 2 days (○), values of G' go through a minimum at ca. 106 °C followed by an increase in G' and then finally start to decrease very rapidly at ca. 140 °C. As will be shown below from SAXS study, SI-57 has spherical microdomains in bcc lattice of PS up to 130 °C, and thus the annealing of SI-57 at 70 °C for 2 days was not sufficiently long for the specimen to achieve an equilibrium morphology. For the specimen annealed at 120 °C for 3 days (△), values of G' do not go through a minimum. For the specimen annealed at 120 °C for 3 days followed by heating to 150 °C and then cooling to 80 °C and held there for 1 h, then cooled to 80 °C and held there for 2 h, values of G' decrease rapidly with increasing temperature, going

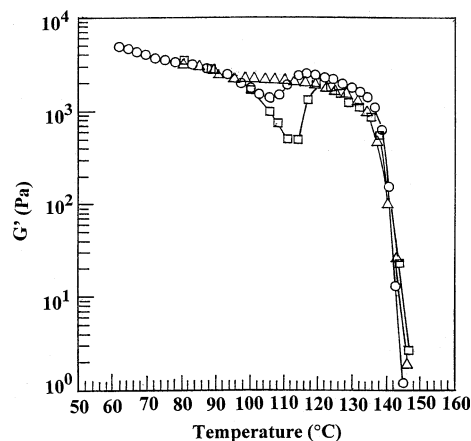


Figure 8. Temperature dependence of dynamic storage modulus G' during heating in the isochronal temperature sweep experiment at $\omega = 0.01$ rad/s for highly asymmetric solvent-cast SI-57 specimens that had the following thermal histories: (○) after annealing at 70 °C for 2 days, (△) after annealing at 120 °C for 3 days, and (□) after annealing at 120 °C for 3 days followed by heating to 150 °C, held there for 1 h, then cooled to 80 °C and held there for 2 h.

through a very large minimum at ca. 114 °C and then increase rapidly going through a maximum at ca. 122 °C followed by a rapid decrease again. As will be shown below from SAXS study, the appearance of a minimum in G' does not represent the onset of OOT, but rather is due to an annealing effect. One may be tempted to conclude from Figure 8 that SI-57 undergoes ODT from the bcc-sphere phase to the micelle-free disordered phase at ca. 140 °C, because values of G' begin to drop very rapidly. To determine whether this is the case, we investigated via TEM, the morphology of SI-57 from room temperature to 160 °C.

Figure 9 gives the TEM images of SI-57 specimens, the thermal histories of which are given in the figure caption. From Figure 9, we make the following observations. SI-57 has spherical microdomains of PS at 90 °C. As the temperature is increased to 120 °C, well-ordered spherical microdomains of PS persist. As the temperature is increased to 140 °C, above which values of G' begin to drop rapidly in the isochronal dynamic temperature sweep experiments (see Figure 8), the spherical microdomain structure still persists. As the temperature is increased further to 160 °C, the spherical microdomains lose long-range order and yet retain a distinct interface, indicative of the presence of disordered micelles.^{17,22–24} Thus, we tentatively conclude that 140 °C, where values of G' begin to drop rapidly in the isochronal dynamic temperature sweep experiments (see Figure 8), represents the T_{LDOT} or T_{ODT} involving the LDOT process of SI-57. According to our previous study,^{23,24} the disordered micelles observed at 160 °C in Figure 9d should disappear at a certain critical temperature when the temperature is increased beyond 160 °C.

Figure 10 gives log G' vs log G'' plots for a solvent-cast SI-57 specimen at various temperatures ranging from 65 to 190 °C. Prior to the rheological measurements the specimen was annealed at 70 °C for 36 h. From Figure 10, we conclude that SI-57 is in the homogeneous state at temperatures approximately 185 °C and higher, where the log G' vs log G'' plot no longer varies with temperature. It is worth noting in Figure 10 that the log G' vs log G'' plot makes a sudden downward shift above 143 °C (▲) giving rise to a slope

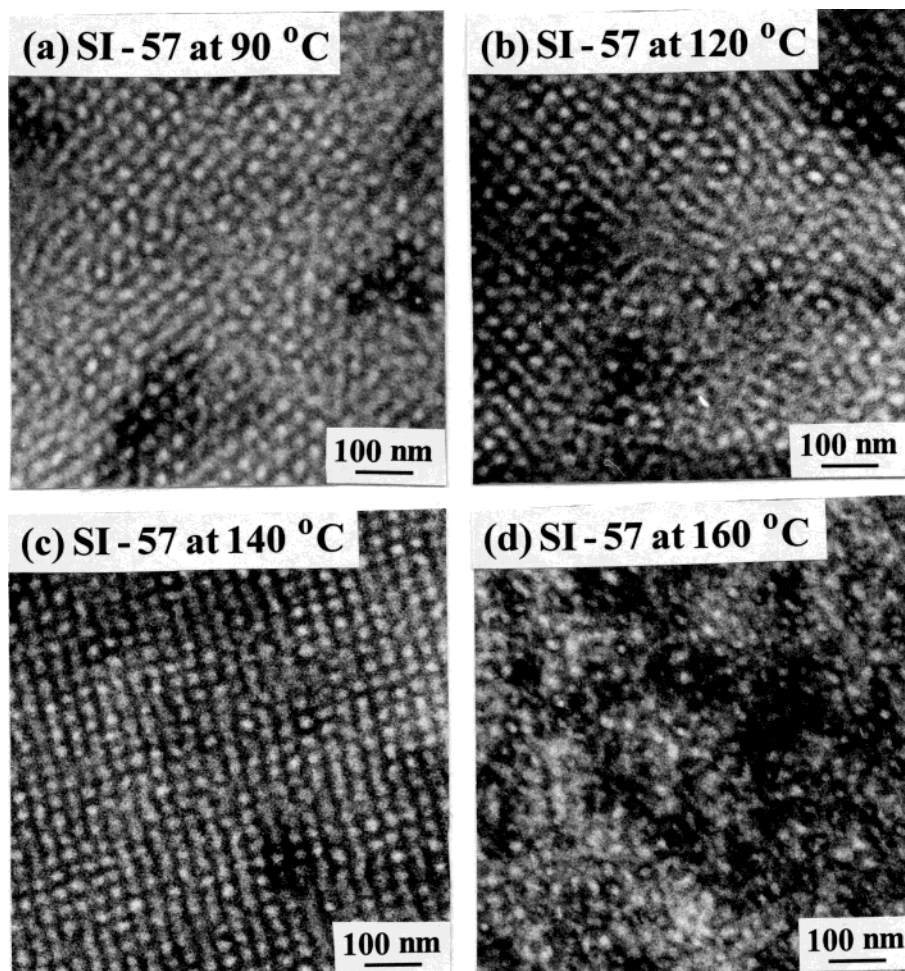


Figure 9. TEM images of highly asymmetric solvent-cast SI-57 specimens: (a) after annealing at 90 °C for 8 days followed by rapid quenching in ice water; (b) after annealing at 120 °C for 3 days followed by rapid quenching in ice water; (c) after annealing at 140 °C for 2 days followed by rapid quenching in ice water; (d) after annealing at 160 °C for 10 h followed by rapid quenching in ice water.

very close to 2 in the terminal region. Thus, we conclude that SI-57 undergoes LDOT at ca. 143 °C and DMT at ca. 185 °C.

The readers are reminded that for symmetric or nearly symmetric block copolymers the temperature at which values of G' begin to drop precipitously from the isochronal dynamic temperature sweep experiment agrees very well with the threshold temperature at which the $\log G'$ vs $\log G''$ plot in the terminal region with a slope of 2 begins to be independent of temperature (see Figures 6 and 7). Notice the distinct differences in the temperature dependence of $\log G'$ vs $\log G''$ plot between the nearly symmetric block copolymers (Figure 6 for SI-13 and Figure 7 for SIS-26) and the highly asymmetric block copolymer (Figure 10 for SI-57), i.e., the $\log G'$ vs $\log G''$ plots for the nearly symmetric block copolymers do *not* exhibit a parallel shift with increasing temperature, whereas the $\log G'$ vs $\log G''$ plots for SI-57 do exhibit a parallel shift with increasing temperature. Thus, we make a distinction between the two situations: one situation where nearly symmetric block copolymer transforms directly into a homogeneous phase with thermally induced composition fluctuations and another situation where highly asymmetric block copolymer first transforms into disordered micelles having liquidlike short-range order at T_{LDOT} and then the disordered micelles transform into the micelle-free

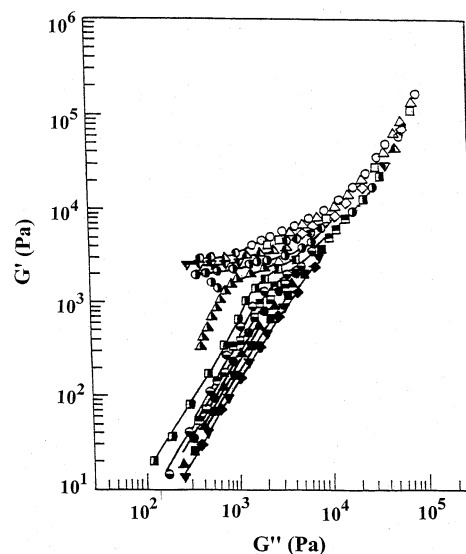


Figure 10. $\log G'$ vs $\log G''$ plots for a highly asymmetric solvent-cast SI-57 specimen during heating at various temperatures: (○) 65 °C; (△) 75 °C; (□) 85 °C; (◇) 103 °C; (●) 109 °C; (▲) 115 °C; (■) 118 °C; (▼) 125 °C; (⊙) 135 °C; (△) 140 °C; (▢) 143 °C; (⊖) 155 °C; (⊞) 160 °C; (⊠) 165 °C; (●) 170 °C; (▲) 175 °C; (■) 180 °C; (▼) 185 °C; (◆) 190 °C. Prior to the rheological measurements, the specimen was annealed at 70 °C for 36 h.

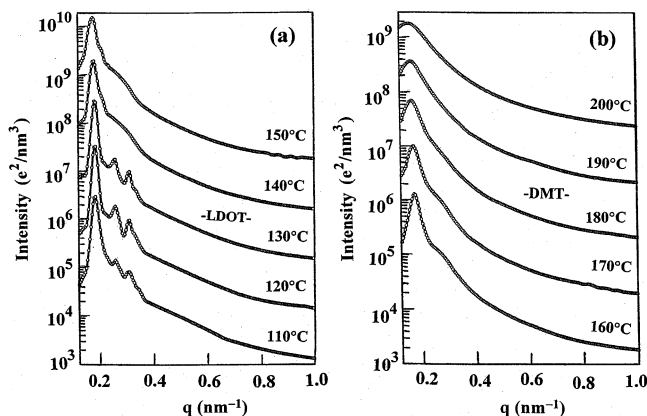


Figure 11. Temperature dependence of desmeared SAXS profiles for a highly asymmetric solvent-cast SI-57 specimen in the heating process at various temperatures: (a) from 110 to 150 °C; (b) from 160 to 200 °C. The intensities of the profiles at 110 °C and 160 °C shown respectively at the bottom of parts a and b of this figure are actually measured absolute values and the intensities of other profiles have been shifted up by one decade relative to the SAXS intensities immediately below. Prior to the SAXS experiment, the specimen was annealed at 70 °C for 36 h.

homogeneous state only with thermally induced composition fluctuations at T_{DMT} .^{23,24}

Figure 11 gives the desmeared SAXS profiles for a solvent-cast SI-57 specimen at various temperatures ranging from 110 to 200 °C in the heating process. Prior to the SAXS experiment, the specimen was annealed at 70 °C for 36 h. The following observations are worth noting in Figure 11. Upon increase in temperature from 110 to 130 °C, we clearly observe the higher order maxima at $q = \sqrt{2}q_m$ and $\sqrt{3}q_m$. This observation indicates that at temperatures below 130 °C, SI-57 exhibits bcc spherical morphology of PS with its long-range order increasing with increasing temperature, which confirms the TEM images given in Figure 9. Upon an increase in temperature from 130 to 140 °C, the SAXS profiles change dramatically, namely the higher order peaks at $q = \sqrt{2}q_m$ and $\sqrt{3}q_m$ disappear and merge into a broad shoulder. This observation indicates that the T_{LDOT} exists between 130 and 140 °C. The value of the T_{LDOT} determined by SAXS is slightly lower than that determined by the isochronal dynamic temperature sweep experiment (see Figure 8). At $T > 140$ °C, we observe both the gradual broadening and the decay of the intensity of the first-order peak. At 140 °C $< T < 180$ °C, the second-order shoulder located at $q \approx 0.3$ nm⁻¹ can be discerned, indicative of the existence of spheres with short-range liquidlike order, as described by the Percus–Yevick theory²⁵ or the paracrystal theory with a large paracrystal lattice distortion of the second type.^{26,27} However, at $T > 190$ °C the second-order shoulder is hard to discern, indicative of the presence of a disordered melt with thermal composition fluctuations but free from disordered micelles. Thus, we determine the T_{DMT} of SI-57 to be 180–190 °C, which is in good agreement with that determined from the $\log G'$ vs $\log G''$ plot (see Figure 10).

Figure 12 gives (a) plots of $1/I_m$ vs $1/T$ and (b) σ_q^2 vs $1/T$ for SI-57 at temperatures ranging from 80 to 200 °C in the heating process, where I_m denotes the first-order peak intensity, σ_q^2 denotes the square of half-width at half-maximum (HWHM), and T denotes the absolute temperature. The following observations are

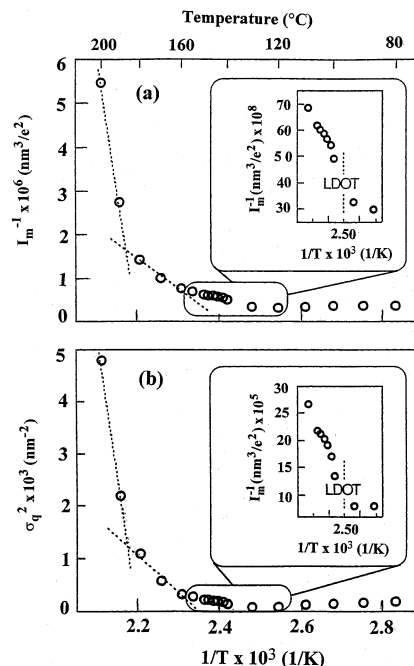


Figure 12. Plots of (a) $1/I_m$ vs $1/T$ and (b) σ_q^2 vs $1/T$ for a highly asymmetric solvent-cast SI-57 specimen in the heating process. Prior to the SAXS experiment, the specimen was annealed at 70 °C for 36 h.

worth noting in Figure 12a: (i) as the temperature is increased from 80 °C, I_m^{-1} first decreases gradually until reaching 130 °C; (ii) there is a small discontinuity of I_m^{-1} as the temperature is increased from 130 to 140 °C, indicating that SI-57 undergoes LDOT at 130–140 °C; (iii) as the temperature is increased from 140 to 200 °C, I_m^{-1} increases steadily. From the intersection of the two dotted lines in the $1/I_m$ vs $1/T$ plot we determine the T_{DMT} of SI-57 to be at 180–190 °C, which is in good agreement with that determined from the $\log G'$ vs $\log G''$ plot (Figure 10). From the σ_q^2 vs $1/T$ plot in Figure 12b, we can make similar observations G' as those made above with reference to the $1/I_m$ vs $1/T$ plot given in Figure 12a. Therefore, we conclude that SI-57 undergoes LDOT at 130–140 °C and DMT at 180–190 °C. The fact (i) given above indicates the improved long-range order of the bcc crystal. Thus, the minimum in the $\log G'$ vs temperature plot given in Figure 8 cannot be due to OOT but is instead due to an annealing effect.

(b) Phase Transition in Highly Asymmetric SIS Triblock Copolymer SIS-110. Figure 13 gives $\log G'$ vs $\log G''$ plots for a solvent-cast SIS-110 specimen at various temperatures ranging from 140 to 214 °C. Prior to the rheological measurements the specimen was annealed at 110 °C for 3 days. The general feature of the temperature dependence of the $\log G'$ vs $\log G''$ plot for SIS-110 is very similar to that given in Figure 10 for SI-57, in that it shows a sudden downward displacement giving rise to a slope very close to 2 in the terminal region and makes a downward parallel shift until reaching a critical temperature at which it begins to show temperature independence. To determine the T_{DMT} of SIS-110 as accurately as possible, the dynamic frequency sweep measurements were taken with an interval of 2 °C from 200 to 214 °C. Because the data points at temperatures above 200 °C given in Figure 13 are too crowded for us to accurately determine the T_{DMT} of SIS-110, we have prepared Figure 14, an enlarged section of the $\log G'$ vs $\log G''$ plots given in

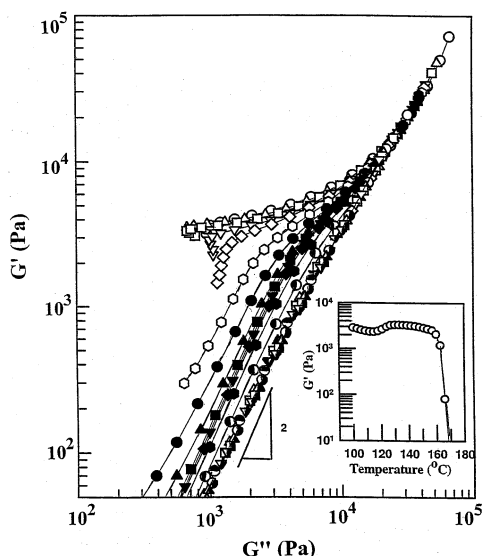


Figure 13. Log G' vs log G'' plots for a highly asymmetric solvent-cast SI-110 specimen during heating at various temperatures: (○) 140 °C; (△) 151 °C; (□) 155 °C; (▽) 160 °C; (◇) 162 °C; (◊) 164 °C; (●) 166 °C; (▲) 168 °C; (■) 170 °C; (▼) 172 °C; (◆) 174 °C; (⊙) 180 °C; (⊖) 190 °C; (△) 200 °C; (▣) 202 °C; (▽) 204 °C; (⊙) 206 °C; (⊖) 208 °C; (△) 210 °C; (▣) 212 °C; (▼) 214 °C. Prior to the rheological measurements, the specimen was annealed at 110 °C for 3 days. The inset describes the temperature dependence of G' obtained from the isochronal dynamic temperature sweep experiment at $\omega = 0.01$ rad/s during heating.

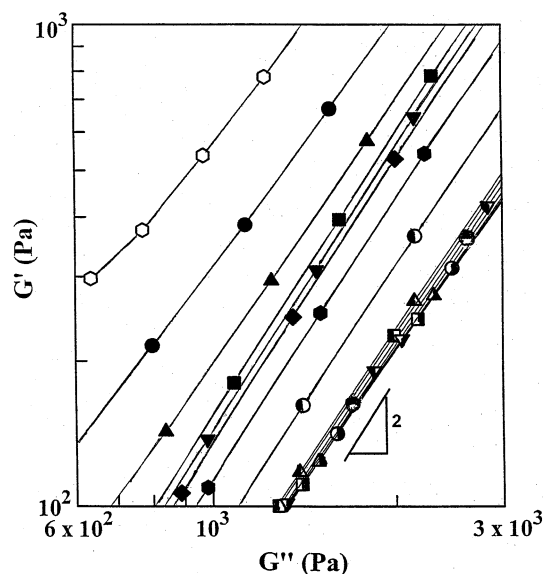


Figure 14. Enlarged section of log G' vs log G'' plots for SIS-110, given in Figure 13, for the values of G' ranging from 10^2 to 10^3 Pa and G'' ranging from 6×10^2 to 3×10^3 Pa at various temperatures: (○) 164 °C; (●) 166 °C; (▲) 168 °C; (■) 170 °C; (▼) 172 °C; (◆) 174 °C; (⊙) 180 °C; (⊖) 190 °C; (△) 200 °C; (▣) 202 °C; (▽) 204 °C; (⊙) 206 °C; (⊖) 208 °C; (△) 210 °C; (▣) 212 °C; (▼) 214 °C. Prior to the rheological measurements, the specimen was annealed at 110 °C for 3 days.

Figure 13, for the values of G' ranging from 10^2 to 10^3 Pa and G'' ranging from 6×10^2 to 3×10^3 Pa. Using the same rheological criterion as that used for Figure 10, from Figure 14 we determine that SIS-110 has T_{LDOT} at 166 ± 2 °C, which is remarkably close to the temperature at which values of G' begin to drop precipitously from the isochronal dynamic temperature measurements (see the inset of Figure 13), and T_{DMT} at 210 ± 2 °C. It is then clear from Figures 13 and 14 that

SIS-110 also undergoes LDOT and DMT in the exactly the same way as SI-57 does. Notice that the T_{LDOT} of SIS-110 is 19 ± 2 °C higher than that of SI-57, and the T_{DMT} of SIS-110 is 23 ± 2 °C higher than that of SI-57. It is interesting to note that the difference in T_{DMT} (i.e., ΔT_{DMT}) between the highly asymmetric triblock copolymer SIS-110 and the highly asymmetric diblock copolymer SI-57 is very close to the difference in T_{ODT} (i.e., ΔT_{ODT}) between symmetric triblock copolymer SIS-26 and the symmetric diblock copolymer SI-13.

Also given in Figure 13 are the results of isochronal dynamic temperature sweep experiments, showing that values of G' go through a minimum at ca. 120 °C, followed by a very mild maximum and then start to decrease precipitously at about 165 °C. This temperature is very close to the threshold temperature at which log G' vs log G'' plots for SIS-110 begin to have a slope of 2 in the terminal region. As observed above in Figures 8 and 10 for SI-57, comparison of the isochronal dynamic temperature sweep data with the dynamic frequency sweep data in Figure 13 suggests that SIS-110 undergoes LDOT at ca. 165 °C. What remains to be seen is whether SIS-110 has disordered micelles at temperature above 165 °C. For this reason, in this study we carried out TEM and SAXS experiments using SIS-110.

Figure 15 gives the TEM images of SIS-110 specimens, the thermal histories of which are given in the figure caption. From Figure 15, we make the following observations. SI-110 has hexagonally packed cylinders of PS at 110 °C. As the temperature is increased to 140 °C, SIS-110 has spherical microdomains in bcc lattice of PS. As the temperature is increased further to 175 °C, the spherical microdomains of SIS-110 have lost long-range order, giving rise to disordered micelles.^{23,24} Notice in Figure 15c that the disordered micelles have a very distinct interface at 175 °C, which lies in the region where log G' vs log G'' plots have parallel features (see Figures 13 and 14), exhibiting liquidlike behavior. Notice that 175 °C is about 10 °C higher than the temperature at which values of G' begin to drop precipitously in the isochronal dynamic temperature sweep experiments (see the inset of Figure 13).

Figure 16 gives the desmeared SAXS profiles for a solvent-cast SIS-110 specimen at various temperatures ranging from 110 to 220 °C in the heating process. Prior to the SAXS experiment, the specimen was annealed at 110 °C for 3 days. The intensities of the SAXS profiles at 110 °C shown at the bottom of Figure 16a and at 164 °C shown at the bottom of Figure 16b are actually measured values, and the intensities of other SAXS profiles have been shifted up by 1 decade relative to intensities immediately below. The following observations are worth noting in Figure 16. At temperatures equal to and below 120 °C, the scattering maxima arising from the interdomain interference exist at the relative peak positions of $1:\sqrt{3}:\sqrt{4}$, indicating the existence of cylindrical microdomains on a hexagonal lattice, which supports the TEM image given in Figure 15a. At temperatures ranging from 130 to 155 °C the SAXS profiles show the scattering maxima at $1:\sqrt{2}:\sqrt{3}$ relative to the first-order maximum, suggesting the existence of spherical microdomains in bcc lattice of PS, which supports the TEM image given in Figure 15b. Above 164 °C, the higher order peaks at $\sqrt{2}$ and $\sqrt{3}$ broaden and overlap into a broad shoulder. Upon increasing temperature further, the broad shoulder becomes broader and less distinct. Finally, the shoulder

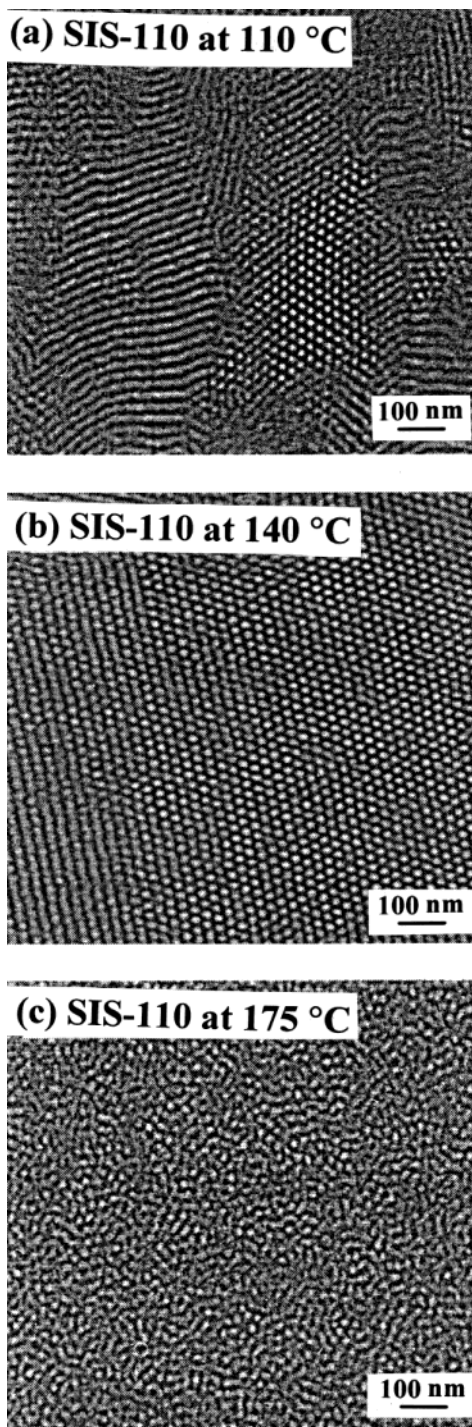


Figure 15. TEM images of highly asymmetric solvent-cast SIS-110 specimens, which had been annealed at 110 °C for 3 days, were annealed further: (a) at 110 °C for 1 h followed by rapid quench in ice water, (b) at 140 °C for 1 h followed by rapid quench in ice water, and (c) at 175 °C for 1 h followed by rapid quench in ice water.

becomes almost indistinguishable. From the SAXS profiles given in Figure 16, we conclude that SIS-110 undergoes OOT from hexagonally packed cylinders to spherical microdomains in bcc lattice of PS at temperatures between 120 and 130 °C, LDOT at temperatures between 155 and 164 °C, and DMT at temperatures between 200 and 205 °C.

Figure 17 gives (a) plots of $1/I_m$ vs $1/T$ and (b) σ_q^2 vs $1/T$, and (c) D vs $1/T$ in the heating process for SIS-110, where D denotes Bragg spacing. The following observa-

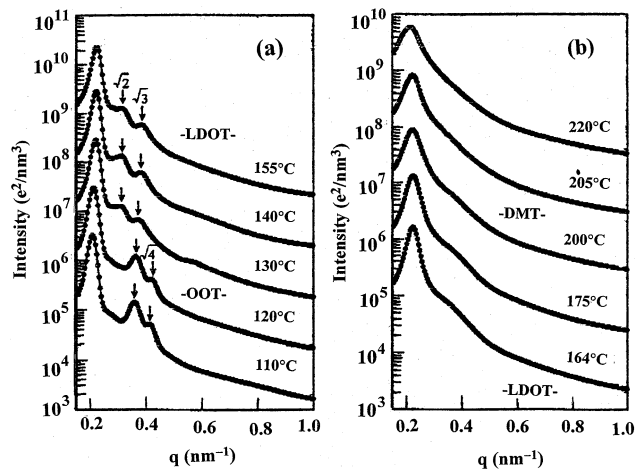


Figure 16. Temperature dependence of desmeared SAXS profiles for a highly asymmetric solvent-cast SIS-110 specimen in the heating process at various temperatures. Prior to the SAXS experiment, the specimen was annealed at 110 °C for 3 days.

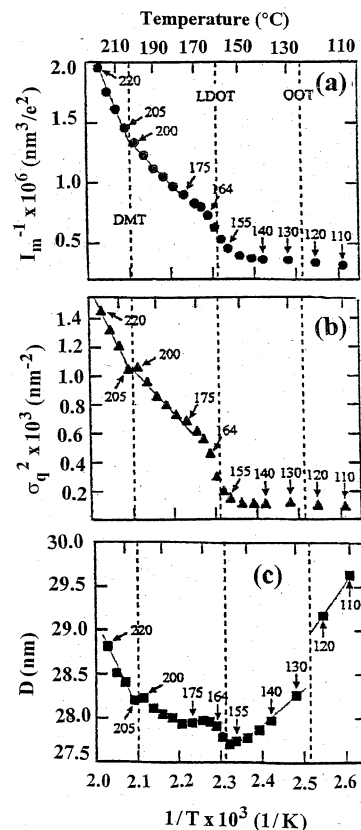


Figure 17. Plots of (a) $1/I_m$ vs $1/T$, (b) σ_q^2 vs $1/T$, and (c) D vs $1/T$ for a highly asymmetric solvent-cast SIS-110 specimen in the heating process. Prior to the SAXS experiment, the specimen was annealed at 110 °C for 3 days.

tions can be made from Figure 17. All three plots in Figure 17 show a discontinuity at temperatures between 155 and 164 °C. These temperatures are best interpreted as representing the onset and completion of LDOT, and the disordered spheres and the bcc-spheres coexist at temperatures between 155 and 164 °C. T_{DMT} is identified by an inflection point in the $1/I_m$ vs $1/T$ and σ_q^2 vs $1/T$ plots.

A large discontinuity at temperatures between 120 and 130 °C shown in the D vs $1/T$ plots indicates OOT, which was identified also from Figure 16.

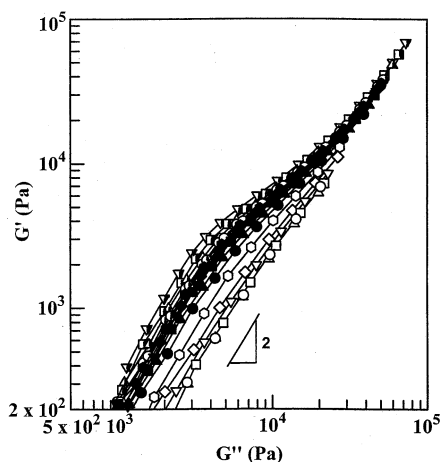


Figure 18. Log G' vs log G'' plots for a highly asymmetric solvent-cast SIS-110 specimen during cooling at various temperatures: (○) 214 °C; (△) 212 °C; (□) 210 °C; (▽) 206 °C; (◇) 200 °C; (○) 190 °C; (●) 180 °C; (▲) 175 °C; (■) 170 °C; (▼) 168 °C; (◆) 166 °C; (●) 164 °C; (○) 162 °C; (●) 160 °C; (▲) 155 °C; (■) 150 °C; (▼) 140 °C. Prior to the rheological measurements, the specimen was annealed at 110 °C for 3 days.

Thermal Reversibility of DMT and Hysteresis Effect of Highly Asymmetric Block Copolymers. Earlier, Schwab and Stuhn²⁸ conducted SAXS experiments on a highly asymmetric SI diblock copolymer during cooling from the homogeneous liquid state, undergoing disorder–order transition that corresponds to LDOT in our terminology. They observed that a stable liquidlike order of micelles existed between the homogeneously disordered state at high temperature and the state of body-centered cubic (bcc) ordered array of spheres at low temperature. They found that upon cooling the size of the spheres increased continuously with decreasing temperature.

In the present study, we conducted, during cooling from the homogeneous liquid state, the dynamic frequency sweep experiments for SIS-110 at various temperatures. Figure 18 gives log G' vs log G'' plots for a solvent-cast SIS-110 specimen at various temperatures during cooling from 214 to 140 °C. Referring to Figure 18, the following observations are worth noting. The data at temperatures ranging from 214 to 210 °C during the cooling process overlap and hence $T_{\text{DMT}} \approx 210$ °C. This temperature is in good agreement, within experimental uncertainties, with the T_{DMT} determined during the heating process. Thus, we conclude that the DMT is thermally reversible under the heating and cooling rates employed in this study. In the temperature range of 140 °C < T < 210 °C, log G' vs log G'' plots are shifted upward with decreasing temperature, keeping a constant slope of 2, and thus system remains in the disordered spheres state, although $T_{\text{LDOT}} \approx 166 \pm 2$ °C in the heating process. Hence the signature of ordering should be seen below 166 °C in the cooling process. This illuminates that the LDOT under the heating and cooling rates employed exhibits the hysteresis, as shown previously by Sakamoto et al.¹⁷ who employed another highly asymmetric SIS triblock copolymer (Vector 4111). In obtaining the results presented in Figure 18, the specimen was cooled stepwise with 2 °C decrements initially and then larger decrements at lower temperatures. Each frequency sweep experiment took about 30 min. As shown in a previous paper of Hashimoto et al.,²⁹ the kinetics of microdomain formation in a block copolymer, upon cooling from the homogeneous

Table 2. Comparison of the Experimentally Determined T_{ODT} of Symmetric AB-Type Diblock and ABA-Type Triblock Copolymers with the Prediction of Mean-Field Theory

sample code	measd T_{ODT} (°C)	ref	predicted T_{ODT} (°C)	
			from the Leibler theory	from the Mayes–Olvera de la Cruz theory
PEP–PEE	75	8	98	
PEP–PEE–PEP	144	8		176
SI	130 ± 1	9	172	
SIS	152 ± 2	9		201
SI-13	86 ± 2	this study	85	
SIS-26	106 ± 2	this study		130

liquid state, is very slow. To minimize hysteresis effect in our experiment, ideally the specimen should have been kept at each measurement temperature for longer than 2–3 h, which however was not feasible, since the entire dynamic frequency sweep experiment during cooling would have then required more than 60 h.

4. Concluding Remarks

In this paper, we have shown that sample preparation methods employed (compression molding vs solvent casting) and the thermal history of specimen have profound influences on the determination of phase transition temperature(s) of highly asymmetric block copolymers. On the basis of the results obtained in this study we recommend the following practice for determining the phase transition temperature(s) of highly asymmetric block copolymers: (i) a slow solvent casting, instead of compression molding, be used to prepare specimens, (ii) optimum annealing conditions in terms of temperature and the duration of annealing be determined, and (iii) sufficiently low angular frequencies (e.g., 0.01 rad/s) be applied to a specimen when conducting isochronal dynamic temperature sweep experiments.

In this paper, we have also shown that the T_{ODT} of symmetric SIS triblock copolymer is ca. 20 °C higher than that of the corresponding SI diblock copolymer, which is in agreement with the previous finding of Riise et al.⁹ But $\Delta T_{\text{ODT}} = 20$ –25 °C between the SIS triblock and SI diblock copolymers is much smaller (approximately one-third) compared to that ($\Delta T_{\text{ODT}} \approx 70$ °C) observed for PEP-*block*-PEE and PEP-*block*-PEE-*block*-PEP copolymers by Gehlsen et al.⁸ In the present study, we have calculated the T_{ODT} of symmetric AB-type diblock copolymers using the mean field theory of Leibler¹ and the T_{ODT} of symmetric ABA-type triblock copolymers using the mean field theory of Mayes and Olvera de la Cruz.⁴ Table 2 gives a summary of the calculations, together with experimental results. For the calculations of the T_{ODTs} summarized in Table 2, the following expressions for the Flory–Huggins interaction parameter were used:

$$\chi = 4.44 \times 10^{-4} + 4.69/T \quad (1)$$

for the PEP-*block*-PEE and PEP-*block*-PEE-*block*-PEP copolymers,³⁰ and

$$\chi = -0.0419 + 38.54/T \quad (2)$$

for the SI diblock and SIS triblock copolymers.³¹ We hasten to point out that predicted values of T_{ODT} depend on the specific expressions for the interaction parameter employed. Nevertheless, it is seen in Table 2 that the experimentally observed trend in ΔT_{ODT} between the

Table 3. Summary of Experimentally Determined T_{LDOT} and T_{DMT} for SI-57 and SIS-110 from $\log G'$ vs $\log G''$ Plots and SAXS

sample code	T_{LDOT} and T_{DMT} determined from $\log G'$ vs $\log G''$ plot	T_{LDOT} and T_{DMT} determined from SAXS
SI-57	$T_{\text{LDOT}} = 143 \pm 2^\circ\text{C}$ $T_{\text{DMT}} = 185 \pm 2^\circ\text{C}$	$T_{\text{LDOT}} = 130\text{--}140^\circ\text{C}$ $T_{\text{DMT}} = 180\text{--}190^\circ\text{C}$
SIS-110	$T_{\text{LDOT}} = 166 \pm 2^\circ\text{C}$ $T_{\text{DMT}} = 208 \pm 2^\circ\text{C}$	$T_{\text{LDOT}} = 155\text{--}164^\circ\text{C}$ $T_{\text{DMT}} = 200\text{--}205^\circ\text{C}$

symmetric triblock and diblock copolymers is predicted by the mean field theories employed.

In this paper, we have shown from oscillatory shear rheometry and SAXS that the highly asymmetric diblock copolymer SI-57 and triblock copolymer SIS-110 undergo LDOT followed by DMT. Table 3 summarizes the values of T_{LDOT} and T_{DMT} for SI-57 and SIS-110 determined from $\log G'$ vs $\log G''$ plot and SAXS experiments, respectively. It is seen in Table 3 that both T_{LDOT} and T_{DMT} of SIS-110 are ca. 20°C higher than those of SI-57. We have demonstrated that the existence of disordered micelles at $T_{\text{LDOT}} \leq T < T_{\text{DMT}}$ is characteristic of highly asymmetric block copolymers, regardless of whether they are diblock or triblock copolymers. From the SAXS experiments performed in the present study on SI-57 and SIS-110, we observe that over a narrow temperature range (less than 5°C) the ordered spheres in bcc lattice coexist with the disordered micelles having short-range liquidlike order. Such observations are supported by an independent TEM study.

At present there is no theory enabling us to predict the T_{LDOT} and T_{DMT} of highly asymmetric block copolymers. Dormidontova and Lodge³² calculated critical micelle temperature (T_{CMT}), which separates the disordered micelle regime from the micelle-free homogeneous phase. They noted that T_{CMT} was significantly higher than T_{ODT} (T_{LDOT} in our terminology). However, they found that the thermodynamic state above and below T_{CMT} was essentially the same, which led them to conclude that disordered micelles might be regarded as being part of the disordered phase. We wish to point out that T_{CMT} defined by Dormidontova and Lodge³² corresponds to T_{DMT} in our terminology. Although we recognize that the currently held mean field approach including the analysis of Dormidontova and Lodge has been quite successful in explaining certain physical phenomena occurring in block copolymers, we are of the opinion that a theory needs to be developed to predict LDOT and DMT in highly asymmetric block copolymers using approaches other than mean field approach.

Before closing we would like to point out that the defect density may vary with the thermal history of block copolymer samples and the presence of the defects would be an important parameter for liquidizing the bcc lattice of the highly asymmetric block copolymers. The higher defect density will facilitate the lattice disordering as shown in this paper. Therefore, it is very important to monitor the defect density of highly asym-

metric block copolymers in order to obtain reproducible T_{LDOT} of such block copolymers.

References and Notes

- (1) Leibler, L. *Macromolecules* **1980**, *13*, 1602.
- (2) Helfand, E.; Wasserman, Z. R. In *Developments in Block Copolymers*; Goodman, I., Ed.; Applied Science: New York, 1982; Chapter 4.
- (3) Mori, K.; Tanaka, H.; Hashimoto, T. *Macromolecules* **1987**, *20*, 381.
- (4) Mayes, A. M.; Olvera de la Cruz, M. *J. Chem. Phys.* **1989**, *91*, 7228.
- (5) Vavasour, J. D.; Whitmore, M. D. *Macromolecules* **1992**, *25*, 5477.
- (6) Matsen, M. W.; Schick, M. *Phys. Rev. Lett.* **1994**, *72*, 2660.
- (7) Hashimoto, T. In *Thermoplastic Elastomers*; Holden, G., Legge, N. R., Quirk, R., Schroeder, H. E., Ed.; Hanser: Munich, Germany, 1996; Chapter 15A.
- (8) Gehlsen, M. D.; Aldmal, K.; Bates, F. S. *Macromolecules* **1992**, *25*, 939.
- (9) Riise, B. L.; Fredrickson, G. H.; Larson, R. G.; Pearson, D. S. *Macromolecules* **1995**, *28*, 7653.
- (10) Adams, J. L.; Graessley, W. W.; Register, R. A. *Macromolecules* **1994**, *27*, 6026.
- (11) Ryu, C. Y.; Lee, M. S.; Hajduk, D. A.; Lodge, T. P. *J. Polym. Sci., Polym. Phys. Ed.* **1997**, *35*, 2811.
- (12) Hashimoto, T.; Suehiro, S.; Shibayama, M.; Saijo, K.; Kawai, H. *Polym. J.* **1981**, *13*, 501.
- (13) Suehiro, S.; Saijo, K.; Ohta, Y.; Hashimoto, T.; Kawai, H. *Anal. Chim. Acta* **1986**, *189*, 41.
- (14) Fujimura, M.; Hashimoto, T.; Kawai, H. *Mem. Fac. Eng., Kyoto Univ.* **1981**, *43* (2), 224.
- (15) Hendricks, R. W. *J. Appl. Crystallogr.* **1972**, *5*, 315.
- (16) Gouinlock, E. V.; Porter, R. S. *Polym. Eng. Sci.* **1977**, *17*, 534.
- (17) Sakamoto, N.; Hashimoto, T.; Han, C. D.; Kim, D.; Vaidya, N. *Macromolecules* **1997**, *30*, 1621.
- (18) Yamaguchi, D.; Hashimoto, T.; Vaidya, N. Y.; Han, C. D. *Macromolecules* **1999**, *32*, 7696.
- (19) Almdal, K.; Koppi, K. A.; Bates, F. S.; Mortensen, K. *Macromolecules* **1992**, *25*, 1743.
- (20) Förster, S.; Khandpur, A. K.; Zhao, J.; Bates, F. S.; Hamley, I. W.; Ryan, A. J.; Bras, W. *Macromolecules* **1994**, *27*, 6922.
- (21) (a) Han, C. D.; Kim, J. J. *Polym. Sci. Polym. Phys. Ed.* **1987**, *25*, 1741. (b) Han, C. D.; Kim, J.; Kim, J. K. *Macromolecules* **1989**, *22*, 383. (c) Han, C. D.; Baek, D. M.; Kim, J. K. *Macromolecules* **1990**, *23*, 561.
- (22) Sakamoto, N.; Hashimoto, T.; Han, C. D.; Kim, D.; Vaidya, N. *Macromolecules* **1997**, *30*, 5321.
- (23) Han, C. D.; Vaidya, N. Y.; Kim, D.; Sakamoto, N.; Hashimoto, T. *Macromolecules* **2000**, *33*, 3767.
- (24) Choi, S.; Lee, K. M.; Han, C. D.; Sota, N.; Hashimoto, T. *Macromolecules* **2003**, *36*, 793.
- (25) Percus, J. K.; Yevick, G. J. *Phys. Rev.* **1958**, *110*, 1.
- (26) Matsuoka, H.; Tanaka, H.; Hashimoto, T.; Ise, N. *Phys. Rev. B* **1987**, *36*, 1754.
- (27) Matsuoka, H.; Tanaka, H.; Hashimoto, T.; Ise, N. *Phys. Rev. B* **1990**, *41*, 3854.
- (28) Schwab, M.; Stühn, B. *Phys. Rev. Lett.* **1996**, *76*, 924.
- (29) Hashimoto, T.; Ogawa, T.; Sakamoto, N.; Ichimiya, M.; Kim, J. K.; Han, C. D. *Polymer* **1998**, *39*, 1573.
- (30) Bates, F. S.; Rosedale, J. H.; Fredrickson, G. H. *J. Chem. Phys.* **1990**, *92*, 6255.
- (31) Hashimoto, T.; Ijichi, Y.; Fetters, L. *J. Chem. Phys.* **1988**, *89*, 2463.
- (32) Dormidontova, E. E.; Lodge, T. P. *Macromolecules* **2001**, *34*, 9143.

MA030116Q